PCCP

Broadband rotational spectroscopy of trans 3-pentenenitrile and 4-pentenenitrile

Journal:	*Physical Chemistry Chemical Physics*
Manuscript ID	CP-ART-08-2019-004328.R2
Article Type:	Paper
Date Submitted by the Author:	11-Oct-2019

Complete List of Authors:	Mishra, Piyush; Purdue University, Department of Chemistry Fritz, Sean; Purdue University, Department of Chemistry Hays, Brian; University of Rennes Mehta-Hurt, Deepali; Johnson and Johnson Vision Jawad, Khadija; Purdue University, Department of Chemistry Zwier, Timothy; Purdue University, Department of Chemistry

Broadband rotational spectroscopy of *trans* 3-pentenenitrile and 4-pentenenitrile

Piyush Mishra, Sean M. Fritz, Brian M. Hays, Deepali N. Mehta-Hurt, Khadija M. Jawad and Timothy S. Zwier*

Department of Chemistry, Purdue University, 560 Oval Drive, West Lafayette, IN 47907, USA

Abstract

Titan, a moon of Saturn, has a nitrogen- and methane-rich atmosphere that is similar to prebiotic earth, and is replete with organic nitriles. Pentenenitriles have not yet been detected in Titan's atmosphere or in molecular clouds, but are potential precursors to hetero-aromatic compounds such as pyridine. We performed broadband microwave studies in the 8-18 GHz range on the *trans* isomer of 3-pentenenitrile (3-PN) and 4-pentenenitrile (4-PN) under jet-cooled conditions. Strong-field coherence breaking (SFCB) was used to selectively modulate the intensities of microwave transitions in a conformer-specific manner for 3-PN, aiding analysis. Two conformers of 3-PN and five conformers of 4-PN were identified and the rotational transitions were assigned. Evidence for methyl internal rotation splitting was observed for both the conformers of 3-PN, and the barrier height of the lowest energy conformer was determined experimentally. Comparison is made of the conformational preferences, stability and isomerization barriers through the acquired rotational spectra and potential energy surface (PES) calculations of the structural isomers 3-PN and 4-PN.

*Author to whom correspondence should be addressed: zwier@purdue.edu

I. Introduction

The list of molecules detected in the interstellar and circumstellar medium continues to grow at an impressive rate of about 4 per year, with some 204 listed in the recent review by McGuire as of late 2018.[1] Among these, -C≡N containing compounds comprise an impressively large fraction (18%), due in part to their large dipole moments and distinctive ^{14}N nuclear quadrupole splittings that make them prime targets for astronomical searches for rotational transitions occurring in the microwave to mm wave regions. Among these are a number of unsaturated nitriles, including long-chain poly-ynes ($HC_{2n+1}N$), CH_2=CH-CN, CH_2=C=CH-CN, and most recently, the aromatic benzonitrile (c-C_6H_5CN).[2] As searches are carried out for even more complicated molecules, it is important to target particular molecules anticipated as likely candidates based on simple reaction sequences.

One logical possibility is that resonance-stabilized radicals, by virtue of their unusual stability, may build up in concentration and subsequently be lost via barrierless radical-radical recombination reactions, which thereby could occur efficiently even at low temperatures. One such recombination reaction of note is that between allyl radical ($^{\cdot}CH_2$-CH=CH_2) and cyanomethyl radical ($^{\cdot}CH_2$-CN) to form 4-pentenenitrile (4-PN) (**Figure 1a**).

$$^{\cdot}CH_2\text{-}CH{=}CH_2 + {}^{\cdot}CH_2\text{-}CN \rightarrow CH_2{=}CH\text{-}CH_2\text{-}CH_2\text{-}CN \text{ (4-PN, } C_5H_7N) \quad (1)$$

Furthermore, given the energetic preference of secondary over primary alkenes, isomerization to 3-pentenenitrile (3-PN) (**Figure 1b**) is exothermic.

$$CH_2{=}CH\text{-}CH_2\text{-}CH_2\text{-}CN \text{ (4-PN)} \rightarrow CH_3CH{=}CH\text{-}CH_2\text{-}CN \text{ (3-PN)} \quad (2)$$

As a result, 4-PN and 3-PN are good candidates to submit to future astronomical searches. However, a first prerequisite for radioastronomy searches are high resolution rotational spectra that can be used to target the search.

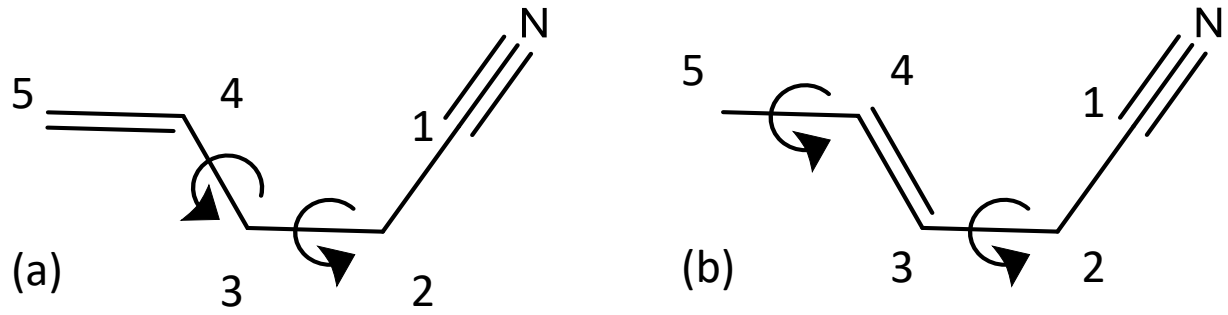

Figure 1: Chemical structures of (a) 4-pentenenitrile and (b) *trans* 3-pentenenitrile molecules. The carbon atoms are labelled starting from the nitrile group and the flexible dihedral angles are indicated.

Nitriles also play an important role in planetary science, most notably in the chemistry of Titan, one of the moons of Saturn. Titan has attracted much attention, as its atmosphere is similar to prebiotic earth.[3] It has a nitrogen abundant atmosphere (>95%), significant methane (3%), and only trace oxygen, rendering it a reducing atmosphere in which organic photochemistry driven by solar radiation plays a dominant role. This photochemistry is initiated by absorption of solar radiation in the vacuum ultraviolet (VUV) region with wavelengths around Lyman α (121 nm) or shorter.[3] This region is energetic enough to break N_2 in the upper atmosphere. CH_4 occurs a little lower in the atmosphere which also photodissociates at VUV wavelengths and reacts with N atoms.[3] Further photochemistry leads to an atmosphere and surface rich in organics (hydrocarbons, aromatics) and especially in nitriles as the principal means of incorporating nitrogen. While the Cassini-Huygens mission provided a remarkable opportunity to characterize the chemical composition of the atmosphere, the recently approved Dragonfly drone mission will characterize the surface composition of Titan in even greater detail, probing the dissolved organics and nitriles that are likely to be abundant there. In laboratory experiments, aerosols thought to be similar to those on Titan (called 'tholins') have been studied in depth and pentenenitriles have been detected by gas chromatography mass spectrometry.[4]

Apart from establishing a database to detect nitrogenous compounds in space, the pentenenitriles are also worthy of attention as potential intermediates along the pathway to heteroaromatics such as pyridine (C_5H_5N). Absorption in the deep UV could provide the energy needed to dissociate them by loss of 2H or H_2, rearrange its backbone, and cyclize to pyridine, either in a single step or in sequence. As the prototypical nitrogen heteroaromatic, establishing pathways to its formation could be important for understanding initial steps along the pathway to nitrogen-rich aromatics present in the nucleic acid bases that are among the fundamental building blocks of life.[5]

Finally, the conformational preferences of 3-PN and 4-PN are interesting in their own right. Both isomers have two C-C single bonds about which torsional motion is possible (**Figure 1**). In 4-PN, these two bonds are adjacent to one another, with torsional motion about the central C2-C3 bond and along C3-C4 due to the non-linear vinyl group. The infrared spectroscopy of 4-PN has been studied under matrix isolated conditions, in the gas phase[6] and the liquid phase[7], and as part of a larger study aimed at understanding the effect of various substituents on the observed vibrational frequencies.

The interior position of the double bond in 3-PN separates the two torsional degrees of freedom, so that the second hindered rotation is that of a methyl group. Furthermore, both *trans* and *cis* isomers are in principle possible, although calculations presented later confirm that the *trans* isomer is significantly more stable. Using Raman and infrared spectroscopy, Durig and co-workers studied the conformational populations of *trans*-3-PN as a function of temperature (-100 to -55°C) in liquid Xe.[8] They concluded that the *syn* conformer (**Figure 2a**) is the global minimum, with the *eclipsed* conformer (**Figure 2b**, labeled 'gauche' by these authors) higher in energy by 205±7 cm^{-1}.

The present work reports the broadband chirped pulse-Fourier transform microwave (CP-FTMW) spectrum of jet-cooled *trans* 3-pentenenitrile and 4-pentenenitrile over the 8-18 GHz range. In order to identify rotational transitions due to individual conformational isomers, the strong-field coherence breaking (SFCB) technique was applied to 3-PN to selectively modulate conformer-specific microwave transitions. Spectra due to the two lowest-energy conformers of 3-PN (*syn* and *eclipsed*) and five of 4-PN were all identified and assigned. Due to the presence of a terminal methyl group adjacent to an sp^2 hybridized carbon in 3-PN, we observed typically small A/E splittings (<1 MHz) due to the two lowest energy methyl internal rotor states. The barriers to internal rotation were experimentally determined for the two conformers of 3-PN. Finally, we compare the conformational landscapes of the two molecules, reflecting on how the conformational complexity will affect searches for rotational transitions of these two nitriles in space.

II. Methods

A. Experimental

The CP-FTMW spectrometer used in this study has been described previously[9,10], hence only the essential aspects will be described here. The spectra were recorded under jet-cooled conditions in the gas phase at rotational temperatures of ~1K. Commercially available 3-PN (95%, Sigma Aldrich), predominantly the *trans* isomer, or 4-PN (97%, Sigma Aldrich) was loaded into a sample reservoir placed immediately before the pulsed valve. 3-PN required no heating, while 4-PN was heated to 70°C to obtain sufficient vapor pressure, and was entrained in helium or argon as backing gases at pressures in the 1.4-3.3 bar range. The gas mixtures were pulsed into a chamber through a pulsed valve (Parker General Valve Series 9) with an orifice of 1 mm diameter operating at 10 Hz. This produced supersonically cooled and isolated molecules in the zero-point levels of the low-lying conformational minima. No evidence for vibrational hot bands was observed in the microwave spectra.. In 3-PN, the different nuclear spin symmetries of the lowest A and E methyl rotor states prevented collisional cooling between them, trapping population in the lowest A and E state.

The CP-FTMW spectrometer, which has been described elsewhere,[9,10] was used to record broadband rotational spectra of 3-PN and 4-PN in the 7.5-18.5 GHz region. Briefly, a 10 gigasamples per second (GS s^{-1}) arbitrary waveform generator (Tektronix AWG7101) was used to generate broadband linear frequency chirps and/or single frequency pulses. The output frequency was up-converted followed by amplification by a 200W travelling wave-tube amplifier (TWTA; Amplifier Research 200T8G18A), which was sent to the vacuum chamber through the broadcasting horn. The microwave pulses intercept the sample molecules, which get polarized and then undergo free induction decay (FID). In order to minimize interference from the microwave pulse, the FID signal was collected by a receiving horn after opening a switch timed to open after a 60 ns delay. The time-domain signal is amplified with a 45 dB low noise amplifier (Miteq AMF-6F-06001800-15-10P), which is down-converted by mixing with an 18.9 GHz PLDRO. Finally, the FID is phase coherently averaged and digitized in the time domain with a 13 GHz, 40 GS s^{-1} real-time digitizer (Guzik ADC6131). Twenty 16 μs long FIDs were collected within each gas pulse, resulting in a resolution of 60 kHz. A Kaiser-Bessel windowing function with a shape parameter of 11.5 was applied to the

molecular FID signal before taking the Fast Fourier Transform (FFT), in order to reduce noise from the TWTA in the early part of the FID. Our experimental resolution limited the internal rotation and the nuclear quadrupolar coupling analysis discussed in the results section; hence, we interpolated the rotational spectra using cubic splines with four times the number of experimental data points (interpolating with three points between consecutive data points) to smooth the spectrum. The maximum intensity of the interpolated lineshapes were used as the line center frequencies of the experimental transitions. This peak picking method led to a reduced average error in the fits of 15 kHz.

For molecules with large dipole moments, chirps from a high power source can operate in the rapid adiabatic passage (RAP) regime where significant population changes are induced by the chirp compared to the weak field limit of linear fast passage (LFP).[11] In order to determine when these conditions were achieved, we recorded preliminary broadband spectra following polarization sweeps from 8 GHz to 18 GHz and from 18 GHz to 8 GHz and collected molecular FIDs at 100%, 10% and 1% of full TWTA power. If the frequency sweep is operating in the RAP regime, population will be moved up or down the rotational ladder by the sweep, producing spectra with different intensities when swept in the two directions.

Anticipating that more than one conformation may be present in the spectrum, we utilized the method of strong-field coherence breaking (SFCB)[9,] to identify a set of transitions due to a single conformational isomer. The SFCB method works best when operating in the RAP regime with strong coupling between the electric field and the molecular dipole moment. SFCB was used systematically only on 3-PN, since the data for this molecule was obtained after the method was more fully developed.

A modified line picking scheme was utilized for 3-PN which is described elsewhere.[9] Initially, an 8-18 GHz chirp followed by a "coherence-breaking" single-frequency pulse (SFP) resonant with the most intense transition in the broadband microwave spectrum was used. A difference spectrum is obtained by subtracting the broadband spectrum from a second broadband spectrum recorded with the SFP present, and plotting the magnitude of the difference between them. Those transitions whose intensities are modulated by the SFP belong to the same conformer as the one targeted by the SFP. Based on those transitions that appear in this difference spectrum, a second transition with a high percent modulation is selected for SFP excitation. The difference spectrum so acquired contains new modulated lines, which are used to choose a third SFP and follow the same procedure to obtain a conformer specific difference spectrum with a sufficient number of intensity-modulated transitions to obtain a preliminary fit to the conformer-specific spectrum. The broadband chirp was 1μs long and the SFPs were each 150 ns long. A gap of 50 ns between the chirp and the first SFP was maintained, while 5 ns gaps between the individual single-frequency pulses was used to avoid beats between them.

Fitting of the 3-PN spectra was complicated by the fact that the magnitude of the nuclear hyperfine and methyl rotor splittings were similar, leading to overlapping transitions that were difficult to deconvolve. As a result, both SPCAT/SPFIT[12] and XIAM[13] program suites were employed in the fitting process. Preliminary fits to the 'A' methyl rotor states were first carried out using SPFIT with a Watson S reduced Hamiltonian which incorporated the nuclear hyperfine splitting, whereas both A and E states along with the hyperfine splittings were fit using XIAM, again with the Watson S reduced Hamiltonian. The best fit rotational parameters and errors from SPFIT were obtained from the PIFORM program available from the PROSPE website.[14]

B. Computational

Calculations were performed using Gaussian 09 suite of programs[15]. Geometry optimizations of all conformational minima of 3-PN and 4-PN were carried out using dispersion-corrected density functional theory with the B3LYP functional (B3LYP-GD3BJ) and the Def2TZVP basis set. This level of theory has

been shown in previous studies to give relative energies in good correspondence with experiment for medium-sized molecules.[9,16,17] Harmonic vibrational frequency calculations were used to obtain zero-point corrected relative energies.

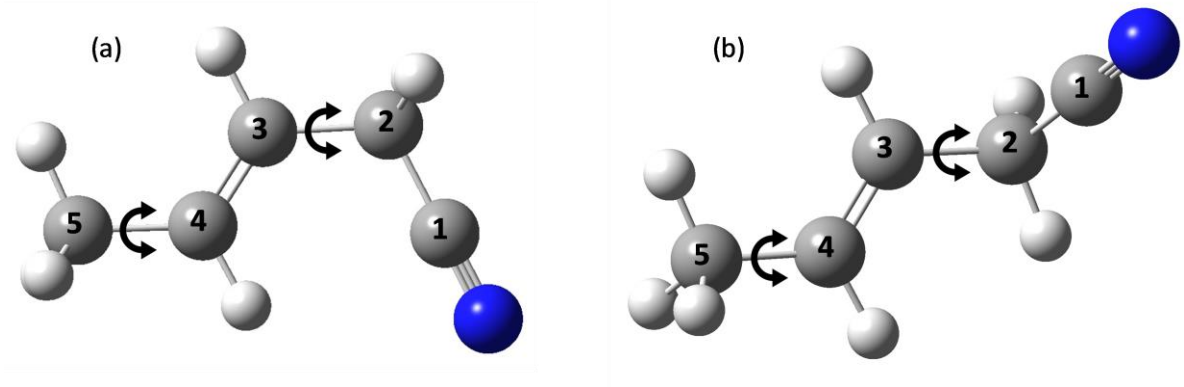

Figure 2: Conformers of *trans* 3-pentenenitrile geometry optimized at the dispersion corrected DFT B3LYP-GD3BJ/Def2TZVP level of theory. The lowest energy conformer (a) *syn* 3-pentenenitrile has all the heavy atoms in the same plane with a C2-C3 dihedral of 0° and (b) *eclipsed* 3-pentenenitrile with a C2-C3 dihedral of -120°, calculated to be 186 cm^{-1} higher in energy. The *eclipsed* conformer exists as a degenerate pair, with its second member having a dihedral angle of +120° (not shown). The flexible dihedral angles are shown as double headed arrows.

The nomenclature followed for 3-PN is based on the C2-C3 dihedral angle, shown in **Figure 2**. The conformer is labelled *syn* when the C2-C3 dihedral θ_{23} has an angle around 0° and *eclipsed* when θ_{23} ~ 120°. Previous studies by Durig and co-workers labelled this second conformer as *gauche* rather than *eclipsed*.[8] Strictly speaking based on IUPAC nomenclature, both the conformers of 3-PN are '*eclipsed*' between the C=C and C-H or C-C(N) bond.[18] However, we distinguish the conformers by the orientation of these groups using '*syn*', a term that denotes that the C=C and C-C(N) bonds are on the same side as opposed to '*eclipsed*' where the C-H bond rotates into that position.

4-PN has two flexible dihedral angles between C2-C3 and C3-C4 as labelled in **Figure 1 (a)**, producing a conformational landscape richer than 3-PN. The Macromodel suite of programs[19] with the generalized AMBER force field was used to identify five conformations for subsequent optimization via DFT. The nomenclature of the 4-PN conformers follows the configuration of the two flexible dihedral angles. For simplicity, the structures are labeled by *e*, *s*, *t*, and *g*, representing *eclipsed*, *syn*, *trans*, and *gauche* respectively. The *e/s* designations follow those in 3-PN, while the C2-C3 dihedral angle is either near 180° (*trans*, *t*) or ±60° (*gauche*, *g*+ or *g*-). Note that *eclipsed* configurations can also take values near ±120°, but these are not differentiated here, as such structures result in mirror images. Further details are in the section where PES analysis is discussed. The nomenclature of the 4-PN conformers labels the C3-C4 dihedral first, followed by the C2-C3 label, as shown in **Figure 3**.

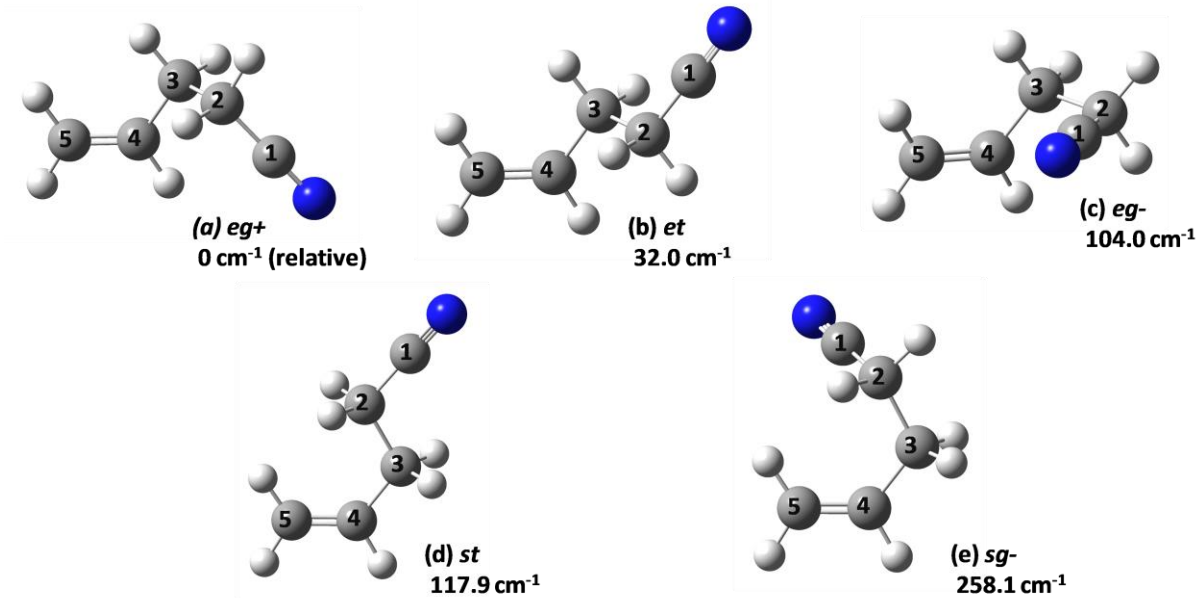

Figure 3: Optimized geometries for the five unique conformers of 4-pentenenitrile calculated at the dispersion corrected DFT B3LYP-GD3BJ/Def2TZVP level of theory. Structures are listed in order of increasing energy: (a) *eg*+, (b) *et*, (c) *eg*-, (d) *st*, and (e) *sg*-. See the text for further discussion of the nomenclature. The relative zero-point corrected energies in cm^{-1} are given below the labels.

Relaxed torsional potential energy curves were calculated along C2-C3 and C4-C5 dihedrals (3-PN) or C2-C3/C3-C4 dihedrals (4-PN) at the same level of theory, in 10° steps. Through this process, we also made sure all possible conformers were obtained along with their degeneracies. In 3-PN, transition state calculations using the quadratic synchronous transit (QST2) method[20] were performed to estimate the zero-point energy (ZPE)-corrected barrier height to methyl rotation.

III. Results

A. 3-pentenenitrile

The DFT calculations of the zero-point corrected relative energies of 3-PN predict that the *syn* conformer (**Figure 2a**) is the most stable, with the *eclipsed* conformer (**Figure 2b**) 186 cm^{-1} (2.23 kJ/mol) higher in energy (**Table 1**). Both conformers are near-prolate asymmetric tops. Broadband microwave spectra of 3-PN were recorded with 1%, 10% and 100% of full microwave power on the TWTA. 3-PN shows clear evidence for distortion of the intensities at full power, as shown in **Figure S1**, and these conditions were used for carrying out SFCB to identify sets of transitions due to conformational isomers. Using the SFCB scheme outlined in Sec. II, we chose transitions at 16773.9375 MHz, 12956.3125 MHz and 10090.0000 MHz as the three single-frequency "coherence-breaking" pulses. These SFPs were subsequently assigned to $5_{1,5}$-$4_{1,4}$, $2_{1,2}$-$1_{0,1}$ and $3_{1,3}$-$2_{1,2}$ transitions of *syn* 3-PN. The final difference spectrum obtained via SFCB exhibited eight peaks whose intensities were modulated by more than 25% by the single-frequency pulses. This difference spectrum, which consisted of a-type and b-type R-branch transitions, is plotted against the simulated fit spectrum of the *syn* conformer in **Figure 4(a)**. Each of the modulated lines was in fact composed of a set of transitions due to ^{14}N hyperfine and methyl rotor splittings, since the 150 ns SFP pulses had widths that subtended these splittings. Based on these transitions, a preliminary fit was

achieved that had rotational constants consistent with those calculated for the *syn* conformer of 3-PN, and transition intensities that reflected its in-plane dipole moment.

Table 1: Zero-point corrected relative energies of the conformers of 3-pentenenitrile and 4-pentenenitrile, calculated at the DFT B3LYP-GD3BJ/Def2TZVP level of theory.

Species	Relative energy (cm^{-1})
3-Pentenenitrile	
Syn	0
Eclipsed	186.3
4-Pentenenitrile	
eg+	0
et	32.0
eg-	104.0
st	117.9
sg-	258.1

Remaining unassigned transitions, presumably belonging to *eclipsed* 3-PN, were about a factor of 10 weaker than those due to the *syn* conformer. SFCB was performed by choosing transitions at 14380.3750 MHz, 17503.0000 MHz and 17023.5000 MHz in subsequent SFCB scans, which were later assigned to the $5_{0,5}$-$4_{0,4}$, $6_{1,5}$-$5_{1,4}$ and $6_{1,6}$-$5_{1,5}$ transitions respectively. In this case, only two additional transitions were identified at a modulation threshold of 35%. A higher percent modulation was required to avoid interference, as the *eclipsed* conformer had transitions that were much weaker than the *syn* conformer. The final SFCB spectrum of the *eclipsed* conformer is plotted against the simulated fit in **Figure 4b**. The transition used for the third SFP was modulated in the previous difference spectrum but its' percent modulation dropped below 35% in the final difference spectrum.

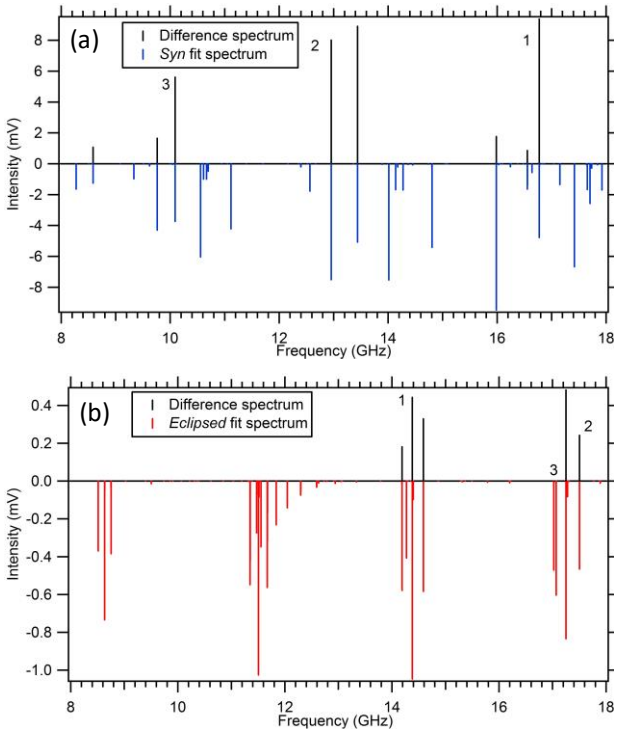

Figure 4: Strong-field coherence breaking spectra of (a) *syn* and (b) *eclipsed* conformers of 3-pentenenitrile (black traces) along with their final fit spectra going down. The intensity axes show almost a factor of 20 difference in signal intensity. The numbering on the transitions label the frequencies of the single frequency pulses of the SFCB method (see text for further discussion).

The broadband microwave spectrum along with the final fit simulation of both the 3-PN conformers is shown in **Figure 5**. The experimental spectrum is a 1M FID average recorded at full TWTA power, with argon as carrier gas at 1.4 bar backing pressure. Final fits were carried out using SPFIT with a Watson-S reduced Hamiltonian. Both these conformers have very low dipole moments along the c axis ($\mu_c \leq 0.1$ D), so only a- and b-type transitions were observed in the spectrum. The final fit is shown in blue. The strong transitions belong to the R branch, and includes both a-type and b-type transitions with similar intensities ($\mu_A \approx \mu_B$).

Figure 6a-c shows three examples of the splittings of individual rotational transitions due to ^{14}N hyperfine and methyl rotor splittings in *syn* 3-PN. The strong a-type lines (e.g., **Figure 6a**) have generally collapsed hyperfine structures with weak side bands, while several of the less-intense a-type transitions have a doublet splitting due to internal rotation. The position of the ^{14}N-atom on the 'a' inertial axis is responsible for collapsing the major hyperfine transitions. By contrast, the b-type lines exhibit hyperfine splittings which are especially clear in the strong transitions (**Figure 6b**). Relatively weaker transitions belonging to Q branch (**Figure 6c**) are also seen consisting of only b-type lines that are broadened doublets with some partially resolved features.

The *eclipsed* conformer of 3-PN (**Figure 2b**) has a structure in which the nitrile group rotates out-of-plane of the other four carbon atoms. In this case, $\mu_b \sim -0.58 \cdot \mu_a$, so the R-branch consists of a-type transitions that are more intense than the assigned b-type transitions. The pattern of hyperfine transitions are much like that in the *syn* conformer, with collapsed structure in the a-type transitions and doublets in the b-type transitions. Weak Q-branch transitions composed only of b-type transitions are also observed. The fit parameters obtained from SPFIT along with the DFT predicted values are listed in **Table 2.** 82 lines of the *syn* conformer were fit (**Table S1)**, while 26 were assigned to the *eclipsed* conformer (**Table S2)**, due to its smaller population and hence weaker transitions. The input fit files corresponding to these conformers are given in the supplementary material.

The conformational population distribution downstream in the supersonic free jet was determined by fitting the rotational transition intensities to Boltzmann plots[21] based on a broadband spectrum taken in the LFP regime with 10% TWTA power with helium backing gas at 1.4 bar. The best-fit plots have T_{rot} = 0.7 K (**Figure S3)** and the population ratio of [eclipsed]/[syn] = 18(10)/82(10) favoring a greater population in the global minimum. Efforts were made to look for the *cis* 3-PN conformer, with calculated energy 631 cm^{-1} (7.55 kJ/mol) above *syn* 3-PN, but no transitions due to this conformer were detected in our spectrum.

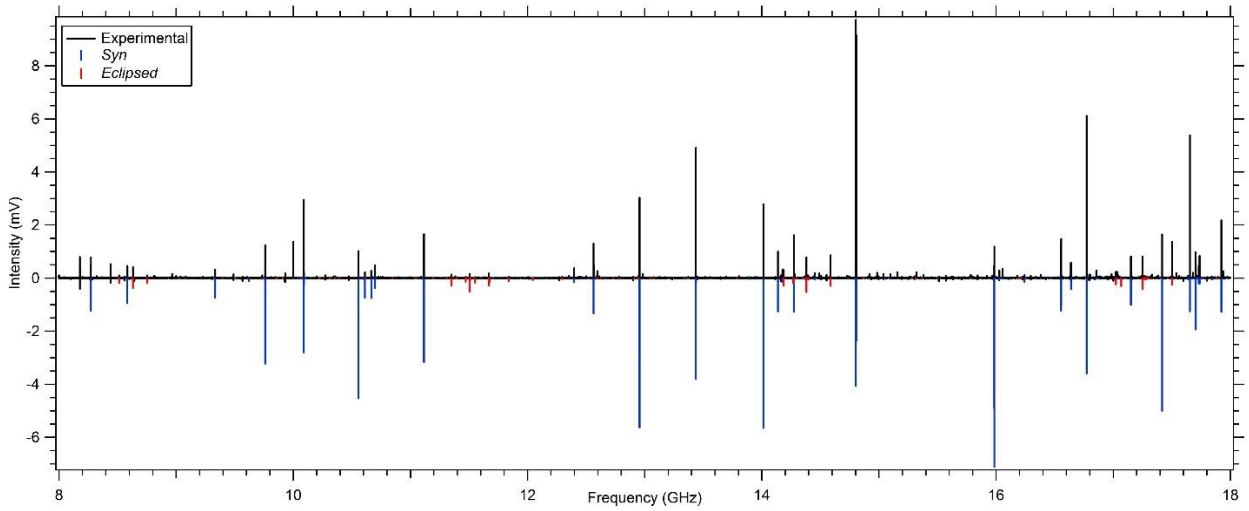

Figure 5: Broadband microwave spectrum of 3-pentenenitrile (black trace) over the 8-18 GHz range with the final fit spectra of *syn* (blue trace) and *eclipsed* (red trace) conformers below. The experimental spectrum is a 1 million average scan of 3-pentenenitrile entrained in argon carrier gas.

Table 2: Spectral fits to the A-state transitions of 3-PN using the SPFIT program suite[12] compared with the values predicted by DFT calculations (Representation I^r Watson S reduction).

3-Pentenenitrile	*Syn*	*Eclipsed*
A (MHz) (pred[a]/expt[b])	8312.7855 / 8163.5900(93)	12901.0547 / 12871.430(23)
B (MHz) (pred/expt)	1926.6016 / 1939.7050(23)	1484.7483 / 1478.8720(47)
C (MHz) (pred/expt)	1594.5939 / 1597.5310(18)	1406.0122 / 1398.9380(34)
μ_A (pred)	2.7	3.8
μ_B (pred)	2.9	-2.2
μ_C (pred)	0.000	0.1
D_J (kHz) (expt)	-0.630(43)	-0.610(60)
D_{JK} (kHz) (expt)	4.40(33)	27.0(19)

χ_{AA} (MHz) (pred/expt)	0.227 / -0.333(07)	-1.934 / 0.73(11)
χ_{BB}-χ_{CC} (MHz) (pred/expt)	-4.810 / -4.760(56)	-2.735 / 2.56(14)
rms (kHz)	25	36
N[c]	82	26
Relative energy (cm^{-1}) (pred)	0	186.3

[a] pred: predicted values at the B3LYP-GD3BJ/Def2TZVP level of theory.

[b] expt: experimental fit values

[c]Number of transitions fit, including individual hyperfine transitions.

B. Methyl internal rotation

The splittings shown in **Figure 6** due to nuclear hyperfine and methyl rotor states were of similar magnitude and led to patterns that were sensitively dependent on the rotational states involved. As a result, fitting both methyl rotor and hyperfine splittings simultaneously was challenging. Moreover, both these types of splittings collapsed at higher J levels for the intense transitions. Since the methyl rotor splittings were just above the experimental resolution of 60 kHz, the error in the derived barrier height is raised.[22,23] Interpolation of the broadband spectra aided in acquiring a better estimation of the frequency of the transitions. In early stages of the fit, we followed previous work, where the hyperfine splitting and internal rotation were treated separately, since the ^{14}N atom responsible for nuclear hyperfine coupling was not in the spatial vicinity of the methyl group.[23,24] The results from these fits were very similar to the final fits (see **Table S3**) The input fit files are included in the supplementary material. As our fits improved, we iteratively alternated between SPFIT to determine A-state hyperfine splittings and XIAM to fit both methyl rotor and hyperfine splittings. This helped ensure that the A and E state transitions were identified properly. After confidently identifying the A and the E states, SPFIT was used to successfully fit the A states, providing high-accuracy rotational constants. Final fits of both nuclear hyperfine and methyl rotor splittings were carried out with XIAM. Representative examples of the fits are shown in **Figure 6a-d**, while a number of additional transitions for *syn* 3-PN are shown in **Figure S2** to illustrate their complexity. The XIAM program was used solely to fit the frequencies and not the intensities of the transitions. As a result, in the predicted stick spectra, the intensity of the E state transitions is taken to be the same as its A state counterpart. The best-fit prediction shown as a stick spectrum in **Figure 6c** are convolved to a Lorentzian lineshape that are overlaid on the stick spectra. With 131 lines fit using XIAM, the lowest energy *syn* conformer of 3-PN has a barrier to methyl internal rotation of 552.9±1.1 cm^{-1} with an average fitting error of 33 kHz. 86 A methyl rotor state transitions and 45 E states were used in the final fit (**Table S4**). The fit parameters from XIAM for *syn* 3-PN are listed in **Table 3**. The corresponding input fit files are given in the supplementary material.

A similar fitting procedure was used to obtain final best-fit rotational parameters in *eclipsed* 3-PN (**Table 3**). The higher energy *eclipsed* conformer of 3-PN has a barrier of 619.4±1.0 cm^{-1} with an average error in the fit of 37 kHz. A total of 32 lines were included in the fit, of which 28 were A states and 4 were E states (**Table S5**). The corresponding input fit files are given in the supplementary material. The transitions due to *eclipsed* 3-PN were much weaker than *syn* 3-PN, moreover the transitions with easily resolved methyl rotor splittings were even weaker, as shown in **Figure 6d**. The best-fit predictions and the convolved Lorentzian lineshape are also shown in **Figure 6d**. Furthermore, all four E states in the fit belonged to R branch a-type transitions with J=4-6 and similar nuclear hyperfine splitting patterns. As a result, while the statistical error in the fits for the two conformers are similar, the extracted methyl rotor barrier height in *eclipsed* 3-PN has a greater risk of systematic error.

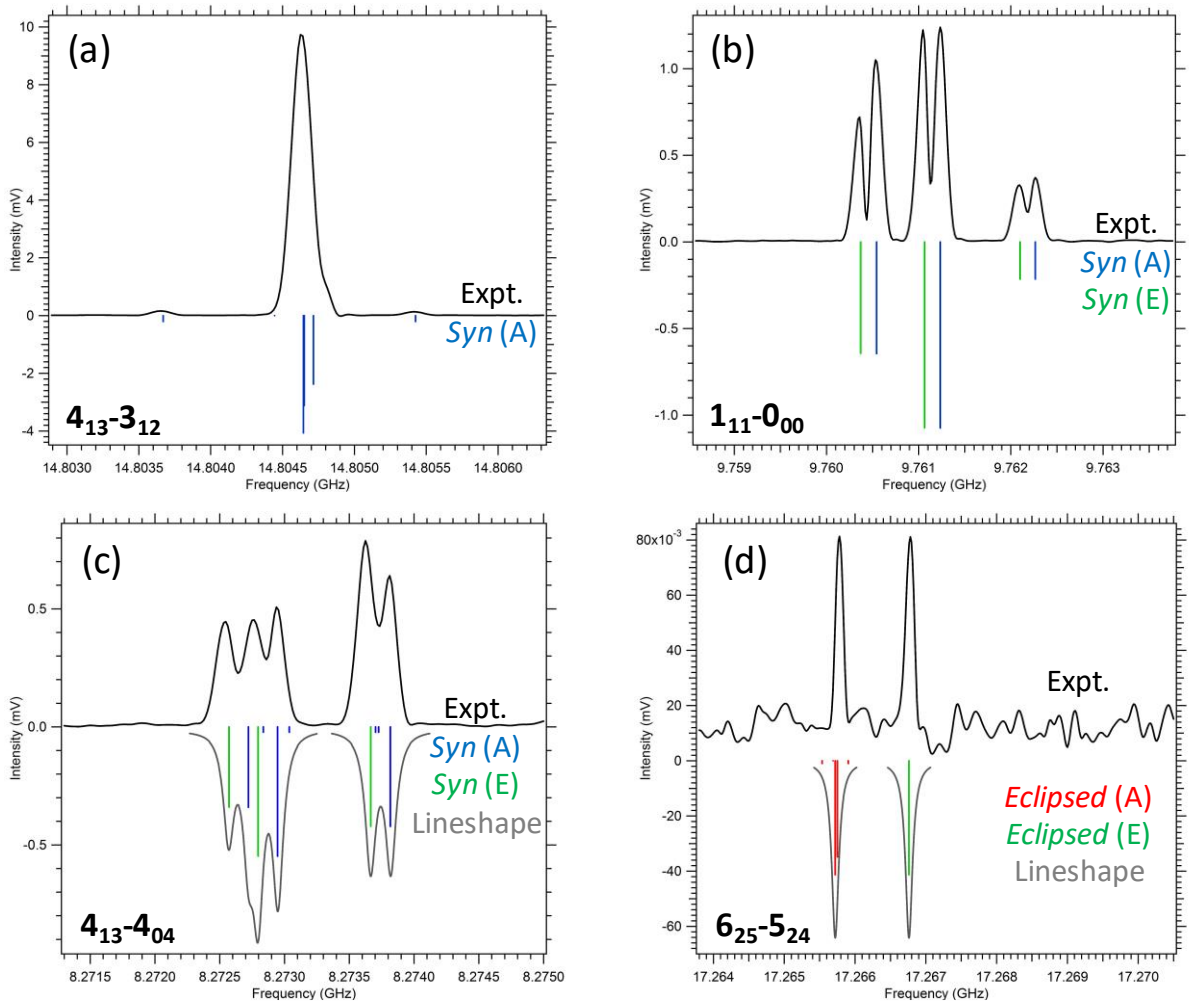

Figure 6: Close-up view of individual transitions of 3-pentenenitrile (black traces) along with the final fits of the A/E states of (a-c) the *syn* conformer (blue/green sticks), and (d) *eclipsed* conformer (red/green sticks). (a) The 4_{13}-3_{12} transition of the *syn* conformer shows collapsed hyperfine splitting with unresolved methyl rotor splittings. The 1_{11}-0_{00} (b) and 4_{13}-4_{04} (c) transitions of the *syn* conformer with both hyperfine and methyl rotor splittings. Predictions of 4_{13}-4_{04} (c) are convolved to Lorentzian lineshapes and are overlaid (grey trace). (d) The 6_{25}-5_{24} transition of the *eclipsed* conformer in which only methyl rotor splittings are resolved. The predicted fits are convolved to Lorentzian lineshapes and are overlaid (grey trace).

Table 3: Spectral fits to both A and E methyl rotor states of 3-PN using the XIAM program suite[13] compared with the values resulting from DFT calculations (Representation I^r Watson S reduction).

3-Pentenenitrile	*Syn*	*Eclipsed*
A (MHz) (pred[a]/expt[b])	8312.7855 / 8163.5733(81)	12901.0547 / 12871.163(16)
B (MHz) (pred/expt)	1926.6016 / 1939.7216(19)	1484.7483 / 1478.8795(32)
C (MHz) (pred/expt)	1594.5939 / 1597.5056(16)	1406.0122 / 1398.9152(29)
F_0 (fixed)	158.0	158.0
D_J (kHz) (expt)	0.663(24)	0.512(42)
D_{JK} (kHz) (expt)	-6.19(12)	-27.87(42)
D_K (kHz) (expt)	33.14(65)	-
d_1 (kHz) (expt)	-0.2075(53)	-
d_2 (kHz) (expt)	-0.0070(18)	-
Dpi2J (expt)	0.00114(28)	-
Dpi2K (expt)	-0.0185(14)	-
Dpi2- (expt)	0.00159(16)	-
δ(fixed)	2.099929695	0.544274057
ε (fixed)	2.612459285	1.090581459
χ_{AA} (MHz) (pred/expt)	0.227 / 0.263(15)	-1.934 / 0.655(57)
χ_{BB}-χ_{CC} (MHz) (pred/expt)	-4.810 / -4.346(20)	-2.735 / 2.707(81)
rms (kHz)	33	37
No. of lines fit (A/E)[c]	86/45	28/4
V_3 (cm^{-1}) (pred/expt[d])	609.3 / 552.9±1.1	588.6 / 619.4±1.0

[a] pred: predicted values at B3LYP-GD3BJ/Def2TZVP

[b] expt: experimental fit values

[c] A/E refers to number of A state lines/number of E state lines fit, including individual hyperfine transitions.

[d]The stated error bars are statistical errors from the fit. Due to the small number of assigned transitions in the *eclipsed* conformer, there is a greater risk of systematic error in the fit.

C. 4-pentenenitrile

The conformational search for 4-PN identified five unique conformers, all of which have relative energies within 300 cm^{-1} of the global minimum (**Table 1**), and therefore may be present in the expansion. All five structures are near-prolate asymmetric tops. The broadband spectrum of **Figure 7** was a 1M scan average recorded at 5% TWTA, which is in the LFP regime. SFCB was not applied to 4-PN, hence, we did not record the microwave spectrum in the RAP regime. The spectrum was recorded with helium as backing gas (P_0 = 1.4 bar) in order to retain population in higher-energy conformers in the expansion, which could be cooled away with heavier bath gases such as Ar.[25] As anticipated, the 4-PN spectrum is more complicated than the 3-PN spectrum, indicative of the presence of transitions due to additional conformers.

Essentially all significant transitions in the spectrum in **Figure 7** could be fit to one of the five lowest-energy conformers of 4-PN shown in **Figure 3**, *eg*+(purple), *et* (green), *eg*- (brown), *st* (blue), and *sg*- (red). The rotational parameters from the best fits are summarized in **Table 4**, where they are compared with the predictions of calculation. **Figure 8** shows close-up views of the hyperfine structure present in the five observed conformers.

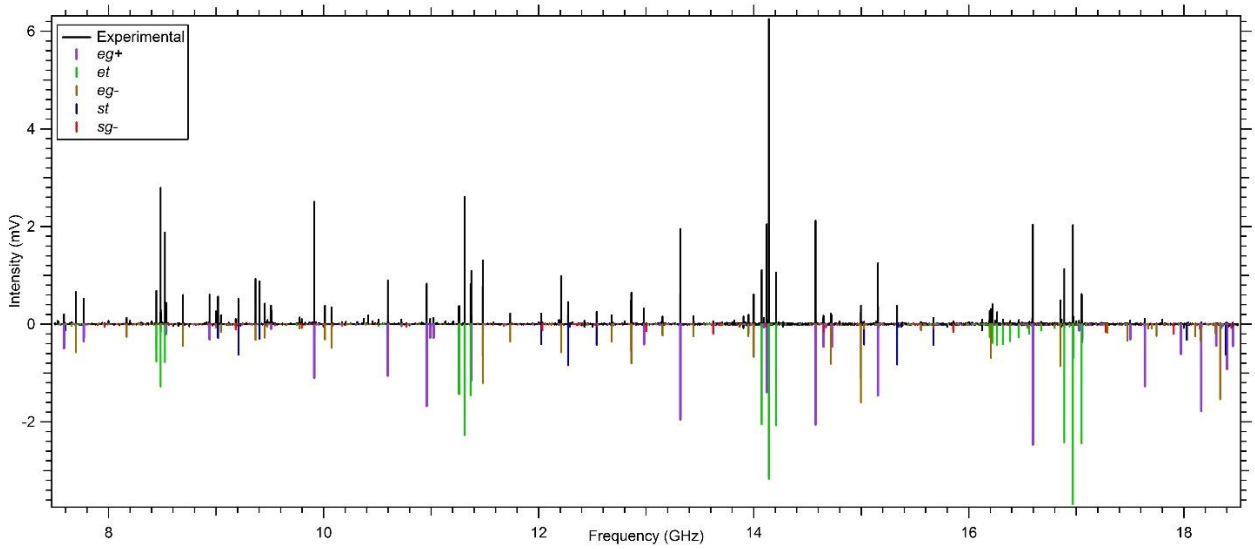

Figure 7: Broadband microwave spectrum in the 7.5-18.5 GHz region of 4-pentenenitrile (black trace) with the final fit spectra of the conformers *eg*+ (violet), *et* (green), *eg*- (brown), *st* (blue) and *sg* (red) shown below. The rotational spectrum is a 1 million FID average of 4-PN entrained in helium carrier gas.

Table 4: Spectral fits using the SPFIT program suite[12] are compared with DFT calculations (Representation I^r Watson A reduction).

4-Pentenenitrile	*eg*+	*et*	*eg*-	*st*	*sg*-
A (MHz) (pred[a]/expt[b])	8297.6034 / 8210.3675(54)	17849.6284 / 17595.7813(56)	5908.6477 / 5804.3411(58)	15041.200 / 14816.7(54)	6008.2593 / 5927.995(11)
B (MHz) (pred/expt)	1952.8733 / 1961.2611(52)	1428.8795 / 1427.6418(13)	2445.7686 / 2491.5640(19)	1600.4804 / 1599.9324(16)	2566.0147 / 2587.2440(34)
C (MHz) (pred/expt)	1700.4463 / 1702.3928(53)	1402.3176 / 1400.6661(15)	1878.9817/ 1892.2972(17)	1472.5354 / 1470.7745(14)	2026.4610 / 2035.7256(51)
μ_A (pred)	2.8	3.9	2.3	4.0	-2.9
μ_B (pred)	2.9	1.3	3.4	0.4	2.8
μ_C (pred)	0.5	0.1	-0.2	0.0	1.1
Δ_J (kHz) (expt)	1.690(47)	0.253(20)	5.001(56)	-	1.77(25)
Δ_{JK} (kHz) (expt)	-21.85(34)	-12.65(30)	-23.38(20)	-	-7.26(63)
Δ_K (kHz) (expt)	102.2(14)	-	40.1(13)	-	-
δ_J (kHz) (expt)	0.3748(94)	-0.0308(76)	1.801(12)	-	-
δ_K (kHz) (expt)	10.9(25)	-	5.58(51)	-	-
χ_{AA} (MHz) (pred/expt)	-0.786 / -0.669(11)	-3.678 / -3.256(11)	0.546 / 0.553 (11)	-4.384 / -3.920(23)	-0.777 / -0.672(25)
χ_{BB}-χ_{CC} (MHz) (pred/expt)	-3.481 / -3.137(20)	-0.930 / -0.863(22)	-5.125 / -4.639(19)	-0.234 / -0.220(48)	-2.402 / -2.208(48)

rms (kHz)	17	19	15	17	17
N[c]	70	70	70	26	24
Relative energy (cm^{-1}) (pred)	0	32.0	104.0	117.9	258.1

[a] pred: predicted values at B3LYP-GD3BJ/Def2TZVP

[b] expt: experimental fit values

[c] N is the number of transitions (including individual hyperfine transitions) in the fit.

The spectrum of the *et* conformer (green) is dominated by triplets of a-type transitions within an R branch, due to a near-prolate asymmetric top. These were the most intense transitions within our spectrum. The transitions display some hyperfine structure, but this structure was largely collapsed, as the ^{14}N atom falls along the a-axis. In addition, a relatively strong Q branch containing b-type transitions was observed in the 16-16.5 GHz range. This Q branch greatly reduced the uncertainty in fitting the A rotation constant, and had well-resolved hyperfine structure, aiding the assignment. Within the Q branch, the hyperfine structure starts to collapse around J=4 at our experimental resolution. As a result, only the Δ_J, Δ_{JK}, and δ_J (kHz) centrifugal distortion terms could be fit reliably.

Transitions due to the *eg*+ conformer, shown in purple, were assigned using patterns resulting from a- and b-type R-branch transitions, but also included a few weak c-type transitions, despite the small value calculated for μ_C (0.5 D). This conformer had the second most intense transitions within the spectrum and several transitions displayed well-resolved hyperfine structure. The fit of the transitions due to the *eg*- conformer, shown in brown, followed similar methods to that for *eg*+; however, in this case, no c-type transitions were observed, likely due to its low predicted dipole moment along this axis. The hyperfine structure was readily apparent in several transitions of this conformer, enabling straight forward assignment of the hyperfine constants. The fits to both these *eg* conformers included Watson-A reduced centrifugal distortion constants.

The *st* conformer, with simulation shown in blue, could be assigned despite its transitions being relatively weak compared to those of the other conformers. Only a-type transitions within an R-branch could be assigned. This branch displayed a largely collapsed hyperfine structure with small hyperfine transitions observable to the sides of each large transition. The assignment of only a-type transitions resulted in a larger uncertainty in the A rotational constant and no centrifugal distortion constants. Searches were conducted for weak b-type transitions but none were observed. This is likely the combined consequence of low population and a weak dipole component along the b-axis (0.4 D).

Finally, the *sg*- conformer, shown in red, was barely observable within the spectrum. As a result, the assignment of the *sg*- conformer could only be accomplished after the assignment of the rest of the spectrum. Accurate predictions of the transition frequencies and hyperfine splittings involving the lowest rotational levels from the DFT calculations played an important role in discerning the transitions in the experimental spectrum. In the final fit, several a- and b-type R-branch transitions could be assigned, including hyperfine splittings that enabled extraction of hyperfine coupling constants (**Table 4**). However, only the Δ_J and Δ_{JK} centrifugal distortion terms could be fit reliably. The linelists of the five 4-PN conformers are in the supplementary material (**Table S6-S10**).

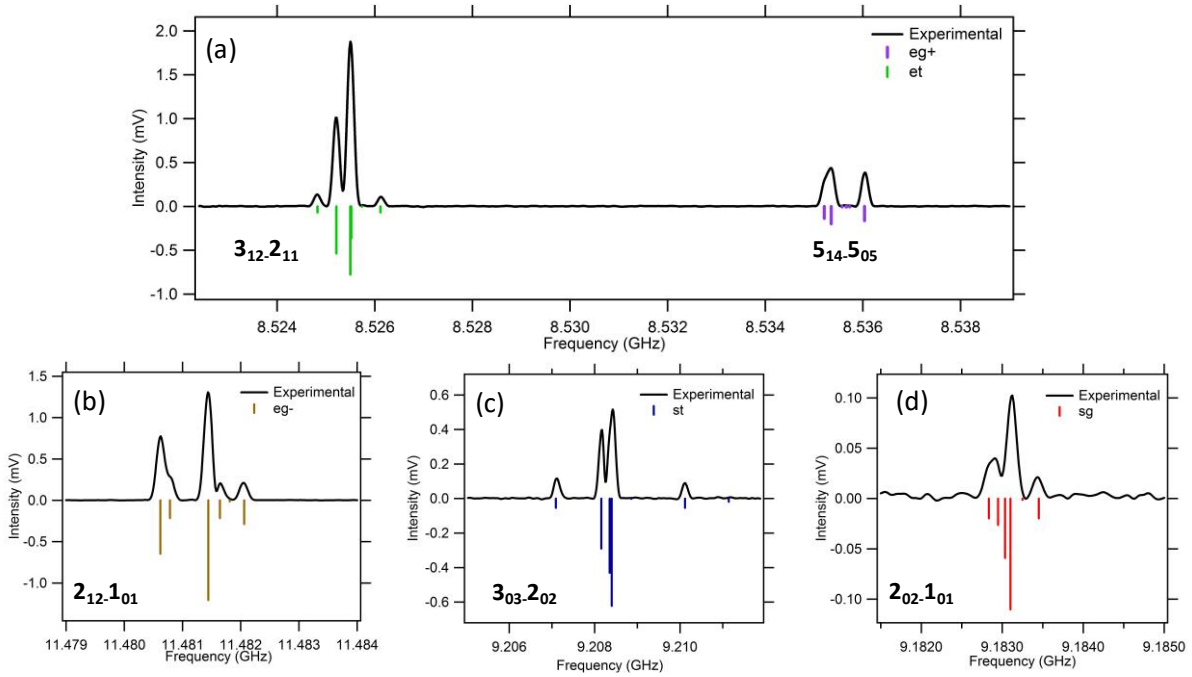

Figure 8: A close-up view of individual transitions of 4-pentenenitrile conformers (black traces) along with their final fit spectra (stick diagrams below). Representative transitions belonging to the (a) *et* and *eg*+ conformers, (b) *eg*-, (c) *st*, and (d) *sg* conformers.

IV. Discussion

A. 3-PN and 4-PN as structural isomers

In the introduction, we conjectured that 4-PN might be anticipated to form in greater abundance in Titan's atmosphere and in molecule-forming regions in space, as it is the recombination product of two resonance-stabilized radicals: allyl ($^{\cdot}CH_2$-CH=CH_2) and cyanomethyl ($^{\cdot}CH_2CN$). However, as a primary alkene, isomerization of 4-PN to the secondary alkene (e.g., 3-PN) is exothermic. This motivated our study of the microwave spectroscopy of this pair of molecules.

3-PN can be formed in both *cis* and *trans* isomers about the double bond. According to the DFT B3LYP-D3BJ/def2TZVP calculations, the *syn* and *eclipsed* conformers of *trans* 3-PN are more stable than the sole conformational minimum (an *eclipsed* structure) in *cis* 3-PN by 631.4 cm^{-1} (7.5 kJ/mol) and 445.1 cm^{-1} (5.3 kJ/mol), respectively. The latter energy difference is similar to the corresponding difference in Δ_fH(0 K) of 4.8 kJ/mol between *cis* and *trans* 2-butene[26], indicating that nitrile substitution on the terminal methyl group is only a minor perturbation on the local energy effects of *cis*-*trans* isomerization about the double bond.

Notably, the corresponding energy difference between primary and secondary alkenes is even larger than the *cis*-*trans* difference. For instance, the global minimum *trans* 3-PN conformer is calculated to be more stable than the global minimum structure of 4-PN by 11.0 kJ/mol (923.5 cm^{-1}), in good correspondence with the Active Thermochemical Tables best values for Δ_fH^o(0 K) that place *trans*-2-butene 11.6 kJ/mol more stable than 1-butene.[26] Again, it would appear that substitution of a terminal nitrile group

has little effect on these energetics. The primary reason for the relative stabilities of these structural isomers can be attributed to hyperconjugation. In case of 3-PN, partial overlap of the out-of plane C-H/C-C σ bonding orbitals occurs from either side of the vinyl group (making it four in total), whereas for 4-PN it occurs only from one side where partial overlap due to two C-H groups is lost, making it less stable than 3-PN (**Figures 2** and **3**).

B. Conformational Preferences of 3-PN and 4-PN

In order to better understand the similarities and differences between the conformational landscapes of 3-PN and 4-PN, we carried out one-dimensional relaxed potential energy scans of the flexible dihedral angles of the two molecules. **Figures 2** and **3** show the optimized conformational structures of the two molecules, keeping the vinyl group fixed in the plane of the page for ready comparison.

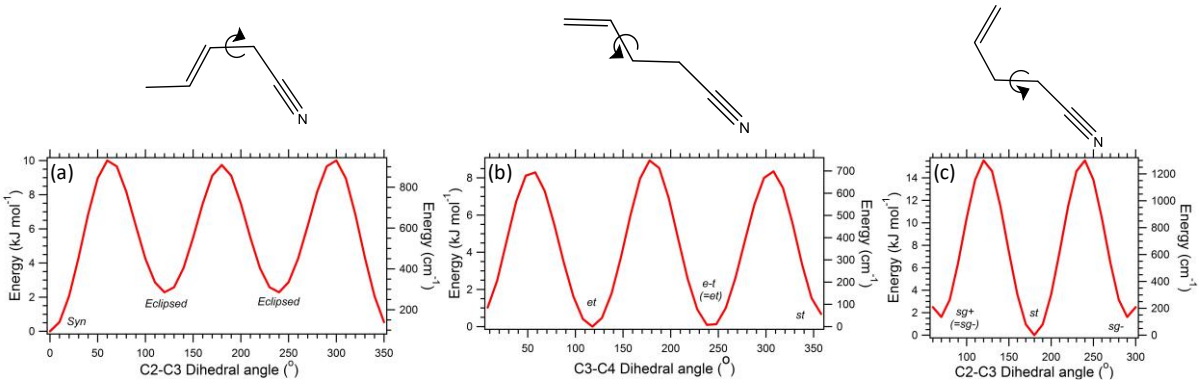

Figure 9: Relaxed potential energy scans of the dihedral angle indicated above it, calculated at the dispersion corrected DFT B3LYP-GD3BJ/Def2TZVP level of theory. (a) The C2-C3 dihedral of 3-pentenenitrile, (b) the C3-C4 dihedral of 4-PN holding C2-C3 in its trans configuration (*xt)*, and (c) the C2-C3 dihedral of 4-PN with C3-C4 held as syn (*sx*). The flexible dihedral angle was rotated in 10° steps. The scan along *sx* includes only dihedral angles from 60 to 300 degrees because the barrier to *sg+*↔*sg-* isomerization is too high due to steric constraints.

Figure 9a shows the relaxed PE curve for 3-PN, stepping along the C2-C3 dihedral, starting from the optimized *syn* geometry. 3-PN has three energy minima, one at the *syn* geometry (defined as 0°), and a degenerate pair of *eclipsed* minima with C2-C3 dihedrals of ±120°. The energetic preference of *syn* over *eclipsed* is born out in our experiment. Not only are the microwave transitions due to the *syn* conformer several times greater than those for the *eclipsed* conformer, but cooling in Ar increases this ratio still further (to near 10, see **Figure 5**), confirming that *syn* is lower in energy than *eclipsed*. This is in keeping with the deduction of Durig and co-workers based on their vibrational spectroscopy in liquid Xe, a non-polar solvent not anticipated to change the gas phase preferences significantly.[8] They determined a $\Delta H_{s\text{-}e}^{o}$ (298.15 K) for the syn→eclipsed isomerization of +2.45 kJ/mol, a value very close to the value predicted by the calculations presented here ($\Delta H_{s\text{-}e}^{o}$ (298.15 K) = +2.34 kJ/mol).

Note that, due to the presence of two *eclipsed* minima (i.e., a degeneracy of 2), $\Delta G_{s\text{-}e}$(298.15 K) = 1.66 kJ/mol, predicting equal populations (i.e., [eclipsed]/[syn] =50/50) at room temperature. This is to be compared with the 18(10):82(10) population ratio of [eclipsed]/[syn] derived from the Boltzmann plots.

This implies that a fraction of the population initially in the *eclipsed* conformational well undergoes collisional cooling over the torsional barrier into the *syn* well during the expansion. The calculated average internal energy of *eclipsed* 3-PN at room temperature is 890 cm^{-1}, while the barrier height for *eclipsed→syn* isomerization is 650 cm^{-1} (**Figure 9a)**, indicating that collision-induced cooling from *eclipsed* to *syn* is energetically feasible. Note that, by comparison, there is no evidence for microwave transitions due to vibrational hot bands of either conformer, consistent with efficient collisional cooling of vibrational energy within a given well.

Arguments based on hyperconjugation can be used to rationalize the energetic preference of *syn* over *eclipsed* in 3-PN. Note, first, that the preferred orientation for the methyl group on one side of the double bond, and the CH_2CN group on the other side, is the same. One C-H/C-C bond lies in plane pointing towards the double bond (**Figure 2a**), while the other two are above and below the plane. Invoking hyperconjugation, this orientational preference involves partial overlap of the two filled σ bonding orbitals on the out-of-plane C-H/C-C(N) bonds with the unfilled π* orbital of the vinyl group.[27] The single in-plane C-H/C-C(N) bond has zero overlap with the π* orbital of the double bond, and thus does not contribute to the stabilization. The *syn* and *eclipsed* conformers differ in the number of out-of-plane C-H and C-C(N) bonds in the CH_2CN group, with *syn* having two out-of-plane C-H bonds, and *eclipsed* one C-H and one C-C(N) bond. But the nitrile group is a strongly electron-withdrawing group, decreasing the electron density in the C-C(N) σ bond, and therefore decreasing its hyperconjugation and stabilization relative to that of a C-H bond. As a result, the *syn* structure is lower in energy than *eclipsed*, as observed and calculated.

The methyl torsional barrier height in 3-PN is also typical of that associated with a $C(sp^3)$-$C(sp^2)$ bond. For instance, we have determined a methyl torsional barrier height for *syn* 3-PN of V_3 = 553 cm^{-1} (6.61 kJ/mol), a value captured to within 10% by the DFT calculations (**Table 3**, V_3=609 cm^{-1} = 7.28 kJ/mol). Previous studies on prototypical molecules like 3-PN, such as acetaldehyde[28] and propene[29] in which a methyl group is attached to a non-aromatic sp^2 hybridized carbon, have deduced barrier heights for methyl internal rotation of 408 cm^{-1} and 684-694 cm^{-1} respectively.

In 4-PN, the two torsionally flexible C-C bonds are adjacent to one another, producing a 2D surface with nine minima, five of which are unique. In our experiment, we have observed all five of these minima, with the most intense transitions (**Figure 7**) assigned to the *et* and *eg+* conformers (green and purple), in keeping with their prediction as the two lowest energy conformers. The *eg-* conformer (brown), calculated to be 104 cm^{-1} higher in energy, has transitions that are third most intense, while the two syn conformers (blue and red) that are calculated as highest in energy, have strongest transitions less than 10% of the most intense bands in the spectrum.

Interestingly, in 4-PN, it is the *eclipsed* conformations *eg+*, *et*, and *eg-*, that are more stable than their *st* and *sg-/sg+* counterparts (**Table 1**) by about 100-150 cm^{-1} (1.2-1.8 kJ/mol). This reversal in conformational preference about the $C(sp^2)$-$C(sp^3)$ bond is a simple consequence of the fact that the nitrile group is moved one bond further away from the vinyl group; hence, hyperconjugation between the $C(sp^2)$ and $C(sp^3)$ carbons is to a CH_2-CH_2 bond rather than CH_2-CN. The electron withdrawing properties of the nitrile group are thus mitigated, and the normal circumstance in which an alkyl group C-C bond undergoes stronger hyperconjugation when out-of-plane than C-H bonds holds. As a result, conformations in which that bond is out-of-plane are preferred, as they are in the *eclipsed* conformers. The experimental rotational temperatures of 4-PN conformers are around 1K (**Figure S4**) with population distribution of *eg+ : et : eg- : st* = 10 : 7 : 7 : 1. The *sg-* conformer has a population smaller than the other four conformers, but could not be quantified.

Relaxed PES scans of 4-PN were carried out for torsional motion about the C3-C4 (**Figure 9(b)**) and C2-C3 dihedrals (**Figure 9(c)**). In the relaxed PES scan along C2-C3 (*sx*), only angles between 60° and 300° were included because the barrier between the *sg+* and *sg-* minima was too high due to steric overlap between vinyl and nitrile groups. The PES scans for *xg+* and *ex* of 4-PN are shown in **Figure S5**. The corresponding scan for *xt* and *sx* were nearly equivalent to the scan in the figure.

The barrier heights for *syn*↔*eclipsed* isomerization along C3(sp^3)-C4(sp^2) are 8-10 kJ mol^{-1}, very similar to the corresponding barrier in 3-PN. By contrast, *gauche*↔*trans* isomerization about the C2(sp^3)-C3(sp^3) dihedral has barriers about twice the size (~17 kJ mol^{-1}, **Fig. 9c**), consistent with a typical torsional barrier in an alkane.[30] We surmise on this basis that isomerization during cooling between *gauche* and *trans* will be quite inefficient, while modest conformational redistribution could occur. A comparison of the relative populations derived experimentally from the rotational Boltzmann plots (**Figure S4**) with the conformers' relative energies show a good qualitative match-up, consistent with small collisional redistribution with helium as buffer gas.

Finally, in the close analog 4-isocyano-1-butene ($H_2C{=}CHCH_2CH_2NC$), which is isoelectronic and isostructural to 4-PN, Samdel *et. al*. found the same three most-abundant conformers as in 4-PN: *et*, *eg+*, and *st* conformers.[31] However, they did not observe the *eg-* and *sg-* conformers, suggesting some differences in the conformational landscape associated with the change of isonitrile for nitrile.

V. Conclusion

Broadband CP-FTMW spectra of 3-PN and 4-PN have been recorded under jet-cooled conditions (T_{rot} ~1 K) over the 8-18 GHz range. 3-PN has a simple conformational landscape with just two conformers, but with the possibility for methyl rotor splittings. Microwave transitions due to both conformers (*syn* and *eclipsed*) have been assigned, including the challenging problem of sorting out methyl rotor/nuclear quadrupole splittings when they are similar in magnitude and just larger than the experimental resolution. 4-PN has five conformers located on a two-dimensional torsional surface with barriers of about 10 kJ/mol for hindered rotation about the C(sp^2)-C(sp^3) and 17 kJ/mol about the C(sp^3)-C(sp^3) axes. All five conformers were observed experimentally, with relative intensities that in large measure follow the relative energies predicted by calculation. The relative stabilities of the 3-PN and 4-PN structural isomers and the preference of *syn* over *eclipsed* in 3-PN can both be understood in terms of hyperconjugation. Here the terminal nitrile group has a relatively minor effect on the relative energies of the structural isomers, but a major effect on the conformational preferences within a molecule.

It is hoped that the present data can provide a foundation for future astronomical searches for these molecules. Of the molecules detected to date in space[1,2], very few have yet had conformational flexibility to them, with n-propyl cyanide and ethyl formate as two notable exceptions.[32] So far, only the lowest energy conformers of the latter two molecules have been detected; however, molecule-forming regions in space have temperatures that may lead to the detection of multiple conformers, and even provide information from their column densities on the mechanisms by which they are formed, and the extent to which thermal equilibrium is maintained.

Acknowledgments

The authors gratefully acknowledge support for this research from the DOE Basic Energy Sciences Gas Phase Chemical Physics program under grant DE- FG02-96ER14656. DNMH and TSZ thank the NASA Planetary Atmospheres program (NNX14AJ47G) for partial support for early phases of the study of 4-PN. PM and SMF carried out the experimental work on 3-PN, while PM did the fitting and wrote a

first draft of the manuscript. Early spectra on 4-PN were taken by DNMH, while BMH recorded additional spectra on 4-PN and did the rotational fitting and analysis. PM and SMF thank Dr. Sven Herbers for useful discussions.

Supplementary Material

See Supplementary material for 8-18 GHz and 18-8 GHz sweeps of 3-Pentenenitrile with 100% power of the TWTA, linelist of the A-states of 3-Pentenenitrile conformers from SPFIT, XIAM fit parameters of 3-Pentenenitrile conformers with hypothetical central frequencies, additional *syn* 3-Pentenenitrile transitions showing hyperfine and methyl rotor splittings, linelist of 3-pentenenitrile conformers from XIAM, linelist of 4-pentenenitrile conformers from SPFIT, Boltzmann plots of 3-pentenenitrile and 4-pentenenitrile conformers to obtain rotational temperatures, PES scans *xg+* and *ex* of 4-Pentenenitrile. The input files corresponding to the linelists are provided in the supplementary material.

References

[1] B. A. McGuire, *Astrophys. J. Suppl. Ser.*, 2018, **239**:17.
[2] B. A. McGuire, A. M. Burkhardt, S. Kalenskii, C. N. Shingledecker, A. J. Remijan, E. Herbst, and M. C. McCarthy, *Science*, 2018, **359**, 202.
[3] F. Raulin, C. Brassé, O. Poch and P. Coll, *Chem. Soc. Rev.*, 2012, **41**, 5380.
[4] M. Morisson, C. Szopa, N. Carrasco, A. Buch and T. Gaurier, *Icarus*, 2016, **277**, 442; M. McGuigan, J. H. Waite, H. Imanaka and R. D. Sacks, *J. Chromatogr. A*, 2006, **1132**, 280.
[5] N. Kitadai, S. Maruyama, *Geoscience Frontiers*, 2018, **9**, 1117.
[6] W. O. George, P. K. Hirani, E. N. Lewis, W. F. Maddams and D. A. Williams, *J. Mol. Struct.*, 1986, **141**, 227.
[7] M. Podzimková, M. Procházka, and M. Paleček, *Collection Czechoslov. Chem. Commun.*, 1969, **34**, 2101; M. Podzimková and M. Procházka, *Collection Czechoslov. Chem. Commun.*, 1970, **35**, 1708.
[8] J. R. Durig, T. K. Gounev, H. Zhen, A. Drew, S. Shen and G. A. Guirgis, *J. Mol. Struct.*, 2000, **553**, 221.
[9] A. O. Hernandez-Castillo, C. Abeysekera, B. M. Hays and T. S. Zwier, *J. Chem. Phys.*, 2016, **145**, 114203; S. M. Fritz, A. O. Hernandez-Castillo, C. Abeysekera, B. M. Hays and T. S. Zwier, *J. Mol. Spectrosc.*, 2018, **349**, 10.
[10] S. M. Fritz, B. M. Hays, A. O. Hernandez-Castillo, C. Abeysekera, and T. S. Zwier, *Rev. Sci. Instrum.*, 2018, **89**, 093101.
[11] D. Schmitz, V. A. Shubert, T. Betz and M. Schnell, *J. Mol. Spectrosc.*, 2012, **280**, 77.
[12] M. Pickett, *J. Mol. Spectrosc.*, 1991, **148**, 371.
[13] H. Hartwig and H. Dreizler, *Z. Naturforsch.*, 1996, **51a**, 923.
[14] PROSPE website: http://www.ifpan.edu.pl/~kisiel/prospe.htm
[15] D. J. Frisch, M. J. Trucks, G.W. Schlegel, H. B. Scuseria, G. E. Robb, M. A. Cheeseman, J. R. Scalmani, G. Barone, V. Mennucci, B. Petersson, G. A. Nakatsuji, H. Caricato, M. Li, X. Hratchian, H. P. Izmaylov, A. F. Bloino, J. Zheng, and G. Sonnenb, GAUSSIAN 09, Revision E.01, 2009, Gaussian, Inc., Wallingford CT.
[16] P. Mishra, D. M. Hewett and T. S. Zwier, *J. Chem. Phys.*, 2018, **148**, 184304.
[17] D. M. Hewett, S. Bocklitz, D. P. Tabor, E. L. Sibert III, M. A. Suhm and T. S. Zwier, *Chem. Sci.* 2017, **8**, 5305.
[18] G. P. Moss, *Pure & Appl. Chem.* 1996, **68**, 2193.
[19] F. Mohamadi, N. G. J. Richards, W. C. Guida, R. Liskamp, M. Lipton, C. Caufield, G. Chang, T. Hendrickson, and W. C. Still, *J. Comput. Chem.* 1990, **11**, 440.
[20] C. Peng, and H. B. Schlegel, *Israel J. Chem.* 1993, **33**, 449.
[21] J. M. Oldham, C. Abeysekera, B. Joalland, L. N, Zack, K. Prozument, I. R. Sims, G. B. Park, R. W. Field, and A. G. Suits, *J. Chem. Phys.*, 2014, **141**, 154202; C. H. Townes, and A. L. Schawlow, *Microwave Spectroscopy*, Dover Publications, New York, 1955.
[22] K. M. Hotopp, V. V. Vara, and B. C. Dian, *J. Mol. Spectrosc.* 2012, **280**, 104.

[23] P. J. Mjöberg, W. M. Ralowski, and S. O. Ljunggren, *Z. Naturforsch.,* 1975, **30a**, 1279.
[24] W. Jäger, and H. Mäder, *Z. Naturforsch.,* 1987, **42a**, 1405; J.-U. Grabow, H. Hartwig, N. Keineking, W. Jäger, H. Mäder, H. W. Nicolaisen, and W. Stahl, *J. Mol. Struct.*, 2002, **612**, 349.
[25] A. Amirav, U. Even, and J. Jortner, *Chem. Phys.*, 1980, **51**, 31.
[26] B. Ruscic and D. H. Bross, Active Thermochemical Tables (ATcT) values based on ver. 1.122e of the Thermochemical Network, Argonne National Laboratory (2019); available at ATcT.anl.gov.
[27] L. G. Wade, *Organic Chemistry*, Pearson, New Jersey, 4th edn. 1999.
[28] I. A. Smirnov, E. A. Alekseev, V. V. Ilyushin, L. Margulés, R. A. Motiyenko, and B. J. Drouin, *J. Mol., Spectrosc.*, 2014, **295**, 44.
[29] J. R. Durig, and G. A. Guirgis, *J. Phys. Chem.*, 1989, **93**, 3489; G. Wlodarczak, J. Demaison, N. Heineking, and A. G. Császár, *J. Mol. Spectrosc*., 1994, **167**, 239; E. Hirota, *J. Chem. Phys.*, 1966, **45**, 1984.
[30] R.G. Ford, *J. Mol. Spectrosc*., 1974, **49**, 117; A. E. Reed, and F. Weinhold *Isr. J. Chem.*, 1991, **31**, 277.
[31] S. Samdal, T. Grønås, H. Møllendal, and Jean-Claude Guillemin, *J. Phys. Chem. A.*, 2014, **118**, 1413.
[32] A. Belloche, R. T. Garrod, H. S. P. Müller, K. M. Menten, C. Comito, and P. Schilke, *Astron. Astrophys.*, 2009, **499**, 215.

Table of contents

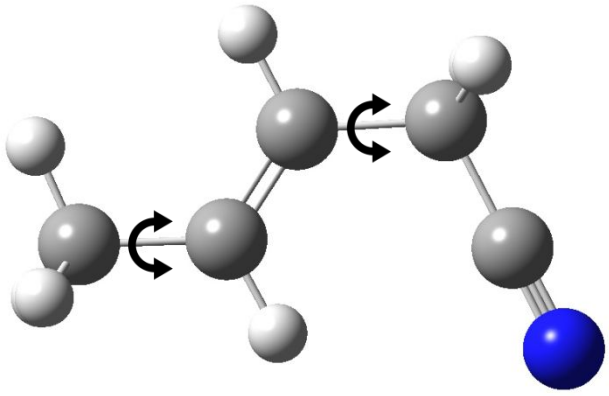

$V_3 = 552.9 \pm 1.1\ cm^{-1}$

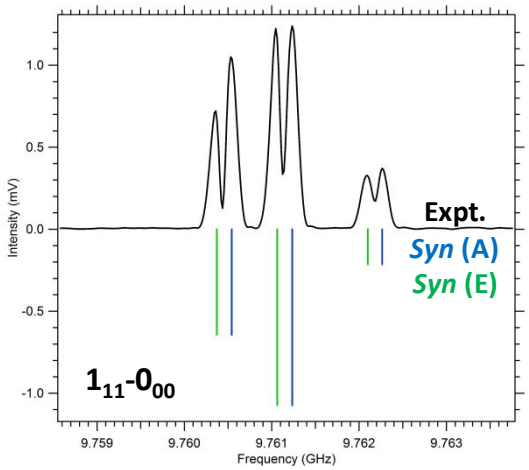

Understanding conformational preferences of 3- and 4-pentenenitriles via broadband microwave spectroscopy.